https://doi.org/10.5194/cp-2023-20
Preprint. Discussion started: 12 April 2023

Climate of the Past Discussions

Equilibrium line altitudes of alpine glaciers suggest summers in Alaska were not more than -2 – -5° C colder than the pre-Industrial during the Last Glacial Maximum

Caleb K. Walcott[1], Jason P. Briner[1], Joseph P. Tulenko[1,2], Stuart M. Evans[3,4]

[1]Department of Geology, University at Buffalo, 126 Cooke Hall, Buffalo, NY, 14260 USA
[2]Berkeley Geochronology Center, Shires Hall, 2455 Ridge Rd, Berkeley, CA 94709 USA
[3]Department of Geography, University at Buffalo, 105 Wilkeson Quad, Buffalo, NY 14261 USA
[4]RENEW Institute, University at Buffalo, 112 Cooke Hall, Buffalo, NY 14260 USA

Correspondence to: Caleb K. Walcott, ckwalcot@buffalo.edu

https://doi.org/10.5194/cp-2023-20
Preprint. Discussion started: 12 April 2023

Climate of the Past Discussions

Abstract

The lack of continental ice sheets in Alaska during the Last Glacial Maximum (LGM; 26 – 19 ka) has long been attributed to arid and relatively warm summer conditions. Records of this aridity across Alaska are relatively abundant, yet quantitative temperature reconstructions have been comparatively lacking until recently. Climate model outputs, a few isolated paleoclimate studies, and global paleoclimate synthesis products show mild summer temperature depressions in Alaska compared to much of the high northern latitudes. This suggests the importance of summer temperature in controlling the relatively limited glacier growth during the LGM. We present a new statewide map of LGM alpine glacier equilibrium line altitudes (ELAs), LGM ΔELAs (LGM ELA anomalies relative to the Little Ice Age [LIA]), and ΔELA-based estimates of temperature depressions across Alaska to assess paleo-precipitation and -temperature conditions. We mapped glacier extents and reconstructed paleoglacier surfaces in ArcGIS to calculate ELAs using an accumulation area ratio (AAR) of 0.58 and an area-altitude balance ratio (AABR) of 1.56. We calculated LGM ELAs (n = 480) across every glaciated massif in the state, excluding areas in southern Alaska that were covered by the Cordilleran Ice Sheet. We see a similar trend of increasing ELAs from the southwest to the northeast during both the LGM and the LIA indicating a consistent southern Bering Sea and northernmost Pacific Ocean precipitation source. Our ΔELAs from the Alaska and Brooks ranges, and the Kigluaik Mountains, average to -355 ± 176 m, well above the global LGM average of ca. -1000 m. Using atmospheric lapse rates, we calculate minimum summer cooling of -3.5 ± 1.7 ºC and maximum summer temperature depressions of -1.9 ± 0.9 ºC. Our results are consistent with a growing number of local proxy reconstructions and global data assimilation syntheses that indicate mild summer temperature across Beringia. Limited summer temperature depressions could be explained by increased incoming solar radiation across

https://doi.org/10.5194/cp-2023-20
Preprint. Discussion started: 12 April 2023

Climate of the Past Discussions

Alaska during the LGM. Limited summer temperature depressions - and general aridity - in Alaska during the LGM have been previously hypothesized as resulting from the complex influence of North American ice sheets on atmospheric circulation.

https://doi.org/10.5194/cp-2023-20
Preprint. Discussion started: 12 April 2023

Climate of the Past
Discussions

1 Introduction

Unlike much of northern North American and western Eurasia, Alaska remained largely free of continental ice sheets throughout the late Pleistocene. Most alpine glaciers and ice sheets across North America reached their late Pleistocene maxima during Marine Isotope Stage 2 (MIS; generally known as the Last Glacial Maximum [LGM]; 26 – 19 ka). However, it has been recognized for decades that ice masses in Alaska reached their greatest extents before this, with comparatively limited glaciation during MIS 2. Early studies hypothesized these maxima occurred during MIS 4 or 6, before absolute age chronologies dated these to MIS 4 (Coulter et al., 1965; Péwé, 1975, 1953; Kaufman et al., 2011; Tulenko et al., 2018). A relative lack of glaciation in Alaska suggests drier conditions and/or milder temperatures during the LGM compared to other parts of the high latitude Northern Hemisphere (i.e., Arctic Canada, western Eurasia, and Greenland). Indeed, researchers have long attributed the lack of large ice sheets to widespread aridity across Alaska (e.g., Hamilton, 1994; Capps, 1932). Other studies also hypothesized that mild temperatures (in addition to arid conditions) led to limited ice sheet development across Alaska (Péwé, 1975; Briner and Kaufman, 2008). If polar amplification (whereby temperature changes in the mid-latitudes are amplified at high-latitudes) operated equally across the Arctic, we would expect Alaska to have experienced greater temperature depressions during the LGM than lower latitude areas of the Northern Hemisphere – thus a dearth of ice sheets would be attributable to a lack of precipitation, rather than warmer temperatures (Miller et al., 2010). However, Alaskan lacustrine paleoclimate proxy studies (e.g., Daniels et al., 2021; Kurek et al., 2009; Finkenbinder et al., 2014; Finkenbinder et al., 2015; Viau et al., 2008; Bartlein et al., 2011; King et al., 2022; Abbott et al., 2010) and global data syntheses (e.g., Osman et al., 2021; Tierney et al., 2020a) suggest that Alaska was comparatively warm and dry during the LGM. Paleoclimate models support mild temperatures in Alaska during the LGM but disagree on whether Alaska was slightly warmer or slightly colder than the pre-industrial period (Löfverström and Liakka, 2016; Löfverström et al., 2014; Otto-Bliesner et al., 2006; Kageyama et al., 2021).

Disagreement between proxy, data assimilation, and model results highlight their respective strengths and weaknesses. Lacustrine proxy data generally offer more ground truth data at a fine resolution, but such studies are time- and labor-intensive and are confined to relatively small geographic areas. Data assimilation products are able to provide broad spatial coverage, but thus far have used marine records to project reconstructed temperatures onto land; though these are compared to terrestrial records, the closest control points to Alaska are in Greenland and may not accurately reflect paleoclimate across Beringia (Osman et al., 2021; Tierney et al., 2020a). Climate models similarly achieve good spatial coverage but lack widespread tie points, useful for evaluating the veracity of certain models. Despite tremendous progress in both data assimilation and climate model development, the lack of terrestrial records highlights a need to provide ground-truth paleoclimate data across large geographic areas – especially in Alaska – where studies suggest surprisingly mild conditions, despite potential polar amplification.

Most of Alaska lacks paleoclimate data coverage due to the general dearth of paleoclimate proxy records statewide that extend back to the LGM. However, we can assess paleoclimate conditions across most of the state by reconstructing equilibrium line altitudes (ELAs) of former glaciers. Glaciers in Alaska were at climatic equilibrium during the Little Ice Age (LIA; ~19th century) before the industrial period and deposited moraines marking their extents, thus serving as a useful pre-industrial climate reference (Barclay et al., 2009; Molnia, 2008; Solomina et al., 2015). Comparing LGM and LIA ELAs allows us to assess relative differences in climate between the two time periods (e.g., Federici et al., 2008).

https://doi.org/10.5194/cp-2023-20
Preprint. Discussion started: 12 April 2023

Climate of the Past Discussions

Here, we present ELA reconstructions for alpine glaciers in Alaska to test the hypothesis that minor temperature depressions – in addition to aridity – explain limited glaciation in Alaska during the LGM. We used the Alaska PaleoGlacier Atlas v2 and high-resolution digital elevation models (DEMs) to map LGM extents, the GlaRe GIS tool to synthesize paleoglacier surfaces, and a GIS ELA calculation tool to evaluate LGM climate (Kaufman et al., 2011; Pellitero et al., 2016; Pellitero et al., 2015). We used similar methods to reconstruct LIA ELAs (and consider this the pre-industrial period) and then calculated ΔELAs and temperature depressions from across the state. We find that distance from a northern Pacific moisture source exercised a strong control on ELAs across Alaska during the LGM and the LIA and our ELA-based paleotemperature reconstructions agree with recent model and paleoclimate data synthesis products showing relatively small LGM temperature depressions in Alaska.

https://doi.org/10.5194/cp-2023-20
Preprint. Discussion started: 12 April 2023

Climate of the Past
Discussions

2 Background

Alpine glaciers are robust indicators of climate as their extent is primarily controlled by summer temperatures and annual precipitation (Ohmura et al., 1992; Ohmura and Boettcher, 2018; Kurowski, 1891; Benn and Lehmkuhl, 2000; Sutherland, 1984; Walcott, 2022; Rupper and Roe, 2008; Roe et al., 2017). Numerous studies have compared ELAs of reconstructed LGM glaciers worldwide to ELAs of extant glaciers (e.g., Kłapyta et al., 2021), ELAs of reconstructed LIA glaciers (Federici et al., 2008), or hypothetical ELAs in the atmosphere (Ono et al., 2005) and used atmospheric lapse rates to estimate LGM temperature depressions. Additionally, several numerical models of alpine paleoglaciers have been developed that quantify paleo-temperature and -precipitation conditions. (e.g., Leonard et al., 2017; Plummer and Phillips, 2003). However, modeling individual alpine glaciers is often time-consuming and computer-intensive and therefore better suited for smaller geographic areas. ELA reconstructions, on the other hand, are relatively labor efficient and more easily applied to a large region (e.g., Brooks et al., 2022; Rea et al., 2020).

Glaciation across Alaska during the LGM was largely restricted to dozens of isolated massifs and mountain ranges across the state, rather than large continental ice sheets seen elsewhere in the Northern Hemisphere (Fig. 1). Much of the Brooks Range was covered by large, interconnected valley glacier systems; poorly constrained drainage divides preclude ELA reconstructions using traditional methods (Kaufman et al., 2011; Hamilton and Porter, 1975). However, numerous valleys outside of the central ice mass in the Brooks Range hosted well-defined cirque and valley glaciers during the LGM. While much of the south-central and southeastern Alaska Range was covered by the Cordilleran Ice Sheet – hampering ELA reconstructions there – there were well-defined and often-extensive glaciers present in the outward-facing (north and west) valleys. The Ahklun Mountains were smothered by an ice cap,

https://doi.org/10.5194/cp-2023-20
Preprint. Discussion started: 12 April 2023

though several portions of the outlying mountains hosted isolated valley glaciers. Outside of these areas, alpine glaciers were present during the LGM within smaller massifs across much of the state from the Yukon-Tanana Uplands to the Seward Peninsula (Péwé, 1975; Coulter et al., 1965; Kaufman et al., 2011).

Present glaciation in Alaska in areas outside of regions of previous Cordilleran Ice Sheet influence are limited (Molnia, 2008; Millan et al., 2022). Extant glaciers beyond central Alaska are present in the Ahklun Mountains, the central Brooks Range, the northern and western Alaska Range, and a lone glacier in the Kigluaik Mountains. These glaciers deposited clear moraines during the LIA, and thus we can calculate ΔELAs (ELA_LIA – ELA_LGM) in these valley systems. We cannot reliably reconstruct ΔELAs in areas where there is a lack of surficial evidence if LIA glaciers, thus precluding us from calculating ΔELAs for every LGM glacier.

Pewé (1975) created a statewide compilation of LGM ELAs using the cirque floor elevation method, where the ELA is assumed to be the elevation of the floor of a cirque. This map revealed a clear west to east rise in ELAs across Alaska, which was later reinforced by subsequent studies from selected areas. In western Alaska, ELAs ranged from ~350 – 600 m asl (Fig. 1; Briner and Kaufman, 2000; Balascio et al., 2005a; Kaufman and Hopkins, 1986). In central Alaska, LGM ELAs were higher, with values of 1530 ± 20 m asl on the Denali massif (Dortch et al., 2010). In eastern Alaska, LGM ELAs reached 1860 m asl (Balascio et al., 2005a). The LGM ELA gradient across Alaska outside of past Cordilleran Ice Sheet influence is hypothesized to have been due to a precipitation gradient similar to today, with higher precipitation in western Alaska and lower precipitation in the eastern part of the state, and the southern Bering Sea and the northernmost Pacific as the dominant moisture sources (Péwé, 1975; Kienholz et al., 2015).

https://doi.org/10.5194/cp-2023-20
Preprint. Discussion started: 12 April 2023

Climate of the Past
Discussions

However, there are two potential issues with these studies. First, the cirque floor elevation method of ELA calculation used by Pewé (1975) has since been suggested to represent a Quaternary average ELA rather than a LGM ELA, as these cirques are eroded across multiple glaciations and often are lower than the actual LGM ELA (e.g., Porter, 1989; Mitchell and Humphries, 2015). Second, the subsequent studies used a variety of ELA calculation methods, making regional patterns somewhat uncertain. Thus, statewide ELA calculations using updated, congruent methods would improve knowledge of LGM ELA trends across Alaska.

Reconstructed LGM ΔELAs from these previous studies range from approximately -200 m to -700 m in the Brooks and Alaska ranges, the Kigluaik and Ahklun mountains, and on Indian Mountain (Hamilton and Porter, 1975; Kaufman and Hopkins, 1986; Balascio et al., 2005a; Briner and Kaufman, 2000; Manley et al., 1997; Péwé, 1975). While these data all consistently highlight a key point – ELA lowering in Alaska during the LGM was less than the average global ca. -1000 m ELA depression – there are some features of previously published studies that we can now build on to create a more congruent dataset (Nesje, 2014; Broecker and Denton, 1990). First, past studies used different contemporary time periods to represent modern glacier ELAs (from different times in the 20th century) as reference points even when Alaskan glaciers were rapidly retreating (Zemp et al., 2019). Second, it is unlikely these modern glaciers were in equilibrium with climate due to this rapid retreat (Molnia, 2008). Third, different methods of ELA calculations of modern and paleoglaciers make direct comparisons more difficult. Fourth, the values from Pewé (1975) likely represent Quaternary average ELAs rather than LGM ELAs. These discrepancies open the door for a comprehensive study to standardize ELA and ΔELA reconstructions across Alaska.

https://doi.org/10.5194/cp-2023-20
Preprint. Discussion started: 12 April 2023

Climate of the Past
Discussions

3 Methods

3.1 Datasets

We employed numerous datasets to calculate LGM and LIA ELAs and ΔELAs. First, we used the Alaska PaleoGlacier Atlas v2 to guide our mapping of LGM ice extents (http://akatlas.geology.buffalo.edu/; date of last access: 1/4/22; Kaufman et al., 2011). We used 1/3 arc-second resolution digital elevation model (DEM) data from the United States Geological Survey (USGS) National Map (https://apps.nationalmap.gov/; date of last access: 1/4/22). To identify LIA moraines, we used false color LANDSAT 8 imagery downloaded from the USGS Earth Explorer (https://earthexplorer.usgs.gov/; date of last access: 1/4/22). Finally, we modern ice thicknesses from Millan et al. (2022).

3.2 Paleoglacier reconstruction

We used the ArcGIS toolbox, GlaRe, in ArcMap 10.8 to recreate 480 LGM and 56 LIA glacier surfaces (Pellitero et al., 2016). The GlaRe toolbox requires a terrain model of the paleoglacier bed, an outline of paleoglacier extent, glacier flowlines, and a user-defined basal shear stress. In valleys with extant glaciers, we created terrain models of paleoglacier beds by simply subtracting modern ice thickness maps from the DEMs (Millan et al., 2022). We identified and mapped the extents of the LGM paleoglaciers from terminal moraines to cirque headwalls in ArcGIS using lateral moraines and trimlines as guides (when present) and were guided by glacier outlines in the Alaska PaleoGlacier Atlas v2 (Kaufman et al., 2011). For large valley glaciers, we used watershed analyses in ArcMap to determine glacier flowlines; for small cirque glaciers, we drew lines from the moraine directly to cirque headwall for simplicity. We calculated ice thickness every 25 m along these flowlines using GlaRe and a standard basal shear stress value of 100 kPa (Benn and

https://doi.org/10.5194/cp-2023-20
Preprint. Discussion started: 12 April 2023

Climate of the Past
Discussions

Hulton, 2010; Pellitero et al., 2016). Using GlaRe, we reconstructed LGM glacier surfaces, using our 'ice-corrected' bed DEMs where appropriate, paleoglacier extent, and flowline ice thickness data as inputs. We repeated these steps for selected valleys with well-defined LIA glaciers outlines. In these locations, we used LANDSAT8 false color imagery to guide LIA moraine mapping.

3.3 Paleoglacier ELA and ΔELA calculation

There are many methods available to calculate paleoglacier ELAs (Pellitero et al., 2015). We chose two of the simplest and most widely used methods: the accumulation area ratio (AAR) and area-altitude balance ratio (AABR). The AAR simply is a ratio between the accumulation and ablation areas of a glacier; we employed a standard ratio of 0.58 (Pellitero et al., 2015; Oien et al., 2021). For the AABR, a climatically controlled mass-balance ratio is applied to glaciers in addition to the areas of the accumulation and ablation zones. The ELA calculated using the AABR is the altitude at which negative and positive mass balances are equal. We employ a ratio of 1.56, which a recent study has found to best represent glaciers worldwide (Oien et al., 2021). We calculated ELAs using LGM and LIA glacier surfaces as inputs to an ELA calculation toolbox in ArcMap (Pellitero et al., 2015). We applied errors of 65.5 and 66.5 m for our AABR- and AAR-calculated ELAs, respectively, as outlined by Oien et al. (2022). To calculate ΔELAs, we simply subtracted LGM ELAs from LIA ELAs for valley systems that hosted glaciers during both periods; errors for these are 131 for AABR and 133 m for AAR to account for the maximum possible errors in ΔELA.

We created trend surfaces for LGM AAR and AABR ELAs across Alaska using the global polynomial tool in ArcMap with polynomial orders from one to four. We also calculated root mean square and X^2 statistics to help determine which polynomial trend surface best described regional

https://doi.org/10.5194/cp-2023-20
Preprint. Discussion started: 12 April 2023

ELA patterns. We excluded southern and southeastern Alaska from our reconstructed surfaces where we did not generate ELA data (Fig. 2)

3.4 Calculating LGM temperature depressions

We applied a range of plausible atmospheric lapse rates to our ΔELAs to calculate LGM temperature depressions following Eq. 1:

$$Temperature\ depression = \Delta ELA \times lapse\ rate \quad (1)$$

where temperature depression is in ºC (and is negative), ΔELA is in kilometers, and lapse rate is in ºC/km. We used the maximum and minimum reported modern-day Alaskan lapse rates of 4.2 and 6.3 ºC/km to calculate temperature depressions (Haugen et al., 1971; Verbyla and Kurkowski, 2019). We consider these maximum temperature depressions as all available evidence suggests Alaska was drier during the LGM than today. (Viau et al., 2008; Bartlein et al., 2011; King et al., 2022; Finkenbinder et al., 2015; Dorfman et al., 2015; Finkenbinder et al., 2014; Muhs et al., 2003; Tierney et al., 2020b; Tierney et al., 2020a; Löfverström and Liakka, 2016; Löfverström et al., 2014). LGM lapse rates are unlikely to have been lower than modern lapse rates because drier air produces smaller magnitude lapse rates. This is because the lapse rate of an air mass increases as it loses its moisture through condensation; therefore, starting with drier air will result in lapse rates that begin to approach the dry adiabatic lapse rate. We also calculated minimum temperature depressions using the dry adiabatic lapse rate of 9.8 ºC/km. The dry adiabatic lapse rate provides a maximum lapse rate for the atmosphere on anything but the shortest timescales (i.e., hours); therefore applying the dry adiabatic lapse rate to our ΔELAs provides a lower limit to our plausible LGM temperature depressions (Kaser and Osmaston, 2002).

https://doi.org/10.5194/cp-2023-20
Preprint. Discussion started: 12 April 2023

Climate of the Past Discussions

4 Results

4.1 Last Glacial Maximum paleoglacier ELAs

Last Glacial Maximum paleoglacier ELAs calculated with AAR ranged from 293 ± 66.5 to 1745 ± 66.5 m asl, while those calculated with AABR were between 306 ± 65.5 and 1742 ± 66.5 m asl (Fig. 2A). While the AAR and AABR vary slightly for the same paleoglaciers, these differences are small (12.5 ± 18 m; 1 σ error reported throughout the manuscript), indicating the veracity of our ELA calculation methods. We report AAR ELAs unless noted, as these calculations do not rely on knowledge of past mass balance gradients (which likely varied across Alaska during the LGM), as required for AABR.

The LGM ELAs values were lowest in the southwestern part of Alaska and highest in northeastern Alaska. In the Ahklun Mountains and surrounding ranges, ELAs were between 293 ± 66.5 and 754 ± 66.5 m asl. Equilibrium line altitudes were also low on the Seward Peninsula (between 370 ± 66.5 and 910 ± 66.5 m asl) and in the western Brooks Range and its sub-ranges (472 ± 66.5 – 1028 ± 66.5 m asl). To the east, ELAs increased across the scattered massifs of the interior, reaching 858 ± 66.5 to 1271 ± 66.5 m asl. Across the Alaska Range, LGM ELAs increased from 929 ± 66.5 m asl in the west to 1589 ± 66.5 m asl in the east. In the Yukon-Tanana Uplands, in eastern Alaska, ELAs were similar, between 1133 ± 66.5 and 1518 ± 66.5 m asl. Finally, we report the highest ELAs in the northeastern Brooks Range, where they reached 1745 ± 66.5 m asl.

4.2 Alaska LGM ELA trend surface

Our calculated LGM trend surface clearly shows increasing ELAs from west to east (Figs. 2B). p-tests applied to the data demonstrate a statistically significant correlation between longitude and

https://doi.org/10.5194/cp-2023-20
Preprint. Discussion started: 12 April 2023

LGM ELAs ($p < 0.01$; Fig. 3). However, we do not find significant correlation between latitude and LGM ELAs (Fig. S1)

4.3 LIA ELAs

We mapped 24 LIA glacier systems; 22 in the Alaska Range, one in the Kigluaik Mountains, and one in the northeastern Brooks Range. Twelve of these valley glacier systems in the Alaska Range hosted multiple LIA glaciers for every LGM glacier. For these systems, we report the mean of all LIA ELAs; these ranged from 1406 ± 66.5 and 1946 ± 66.5 m asl. We calculated an ELA of 1950 ± 66.5 m asl for a LIA glacier on the western side of Mt. Osborn in the Kigluaik Mountains (Seward Peninsula). On the north slopes of Mt. Hubley in the Romanzof Mountains in the northeastern Brooks Range, we calculated an average LIA ELA of 1857 ± 66.5 m asl. These LIA ELAs exhibit a similar trend to the LGM ELAs, with a statistically significant relationship between longitude and LIA ELA ($p < 0.01$; Fig. 4)

4.4 LGM ΔELAs and summer temperature depressions

In the Alaska Range, LGM ΔELAs were between -42 ± 133 m (note that these are standard errors after Oien et al., (2022), but because LGM glaciers were more extensive than LIA glaciers, the positive ΔELAs indicated by the error are implausible. Thus, in these instances, we assume the maximum possible ΔELA is 0 m) and -712 ± 133 m, with a median of -379 m and a mean of -355 ± 180 m (Fig. 4). The ΔELA for our Brooks Range site was -243 m ± 133 m and was -236 m ± 133 m in the Kigluaik Mountains. Median statewide ΔELAs were -335 m, with a mean ΔELA of -345 ± 177 m. We see no statistical relationship between longitude and ΔELA (Fig. S3)

https://doi.org/10.5194/cp-2023-20
Preprint. Discussion started: 12 April 2023

Climate of the Past Discussions

Summer temperature depressions (n = 25) across Alaska calculated with the lowest modern lapse rate estimate ranged between -0.2 ± 1.0 (as above, positive temperature anomalies are implausible based on our methods as ΔELAs do not exceed 0 m) to -3.0 ± 0.6 ºC (median: -1.4 ºC; mean: -1.4 ± 0.8 ºC). These (n = 25) calculated with the highest modern lapse rate estimate range from -0.3 ± 1.4 to -4.5 ± 0.8 ºC (median: -2.1 ºC; mean: -2.2 ºC ± 1.1 ºC). Statewide temperature depressions (n = 25) calculated with the dry adiabatic lapse rate range between -0.4 ± 2.2 and -7.0 ± 1.3 ºC (median: -3.3 ºC; mean: -3.4 ± 1.8 ºC) .

5 Discussion

5.1 Comparisons with Previous Last Glacial Maximum Equilibrium Line Altitude Reconstructions

Our calculated ELAs are generally consistent with those from previous studies. Our ELAs from across the Brooks Range broadly agree with those reported by Balascio et al. (2005a). Their study also reported a maximum Brooks Range ELA of 1860 m asl in the Romanzof Mountains, where we too calculated a statewide maximum ELA of 1745 ± 66.5 m asl. On the Seward Peninsula, our ELAs are generally slightly higher than those previously reported (Kaufman and Hopkins, 1986). In the York Mountains, Kaufman and Hopkins (1986) calculated a single LGM ELA of 370 m asl – we present an average LGM ELA here of 477 ± 85 m asl (n = 5). In the Kigluaik Mountains Kaufman and Hopkins (1986) reported LGM ELAs averaging to 470 m asl (n = 2), falling just outside 1σ of our mean LGM ELA for the Kigluaik Mountains of 585 ± 91 m (n = 64). However, their previously estimated average LGM ELA for the Bendeleben and Darby mountains of 630 m asl matches well with our mean LGM ELA of 657 ± 86 m asl. These slight discrepancies in ELAs between the data is likely attributable to differences in ELA calculation;

https://doi.org/10.5194/cp-2023-20
Preprint. Discussion started: 12 April 2023

Kaufman and Hopkins (1986) used the toe-to-headwall area ratio method of ELA calculation using topographic maps, which has since fallen out of widespread use (Nesje, 2014).

Previous studies in the Ahklun Mountains report LGM ELAs ranging 390 ± 100 m asl and 540 ± 140 m asl, respectively, both overlapping with our mean LGM ELA of 472 ± 117 m asl (Briner and Kaufman, 2000; Manley et al., 1997). Dortch et al. (2010) computed an average LGM ELA from the Peters and Muldrow glaciers near Denali in the central Alaska Range of 1530 ± 20 m asl, which is a few hundred meters higher than our average ELA from the central Alaska Range of 1267 ± 145 m asl; this difference might be attributable to different choices in AAR and AABR ratios, and not correcting for modern ice thickness in glacier surface reconstruction. Finally, LGM ELAs reported by Pewé (1975) are generally slightly higher than our reconstructed ELAs. This is likely due to discrepancies in ELA calculation methods. Pewé (1975) employed the cirque floor elevation method and noted that ELAs calculated thus were systematically higher than those derived with AAR.

We find that our average statewide ΔELAs of -355 ± 180 m, and our ΔELAs for individual ranges generally match previously published ΔELAs from across the state that ranged between -200 and – 700 m (Balascio et al., 2005a; Hamilton and Porter, 1975; Dortch et al., 2010; Briner and Kaufman, 2000; Mann and Peteet, 1994; Péwé, 1975; Kaufman and Hopkins, 1986). These previous data all fall within the range of our average statewide LGM ΔELA, and none approach the global average modern to LGM ΔELA of -1000 m. Though previous studies exclusively used modern ELAs as a reference point for calculating ΔELAs and these glaciers may have been in states of disequilibrium, these still provide useful maximum ΔELA constraints, as LIA ELAs would have been some amount lower than those of modern glaciers, given that LIA moraines are found outside the extents of extant glaciers. Indeed, the most recent studies indicate that maximum

https://doi.org/10.5194/cp-2023-20
Preprint. Discussion started: 12 April 2023

LIA lowering was between 22 and 83 m relative to modern across Alaska (Barclay et al., 2009; Daigle and Kaufman, 2009; Levy et al., 2004; Mckay and Kaufman, 2009; Sikorski et al., 2009). Even when accounting for these LIA ELA depressions, our calculated LGM depressions do not approach the canonical global modern-LGM ΔELA of -1000 m.

We suggest the comparatively minor LGM ΔELAs in Alaska relative to the global average can be attributed to both increased aridity and relatively small summertime temperature depressions. As an example, the tropical Andes both hosted alpine glaciers and experienced conditions more arid today during the LGM. Unlike Alaska, LGM ΔELAs here were near, or greater than, the global LGM ΔELA (Rodbell, 1992; Stansell et al., 2007). Assuming no change in temperature from modern, drier LGM conditions would suggest that LGM glaciers in the tropical Andes should have been smaller than today. However, these LGM glaciers were more extensive than modern due to large temperature depressions at high altitudes that allowed the glaciers to grow, such that their LGM ΔELAs were near the global average (e.g., (Rodbell, 1992; Stansell et al., 2007). Conversely, in Alaska, where the climate was also drier during the LGM than the LIA, low ΔELAs are likely attributable to relatively small LGM temperature depressions. Last Glacial Maximum glaciers in Alaska were larger than the LIA, indicating some amount of temperature depression, but unlike in the tropical Andes, this must have not been large enough to depress LGM ELAs by the global average of ~-1000 m. Indeed, LGM paleoclimate records of aridity and summer temperature from Alaska suggest conditions conducive to this: decreased annual precipitation and summers only slightly cooler than the LIA and much warmer than most of the high latitude regions of the Northern Hemisphere.

https://doi.org/10.5194/cp-2023-20
Preprint. Discussion started: 12 April 2023

Climate of the Past
Discussions

5.2 ELA trends across Alaska

The gradient of LGM ELAs rising eastward agrees well with the previous statewide ELA reconstruction (Péwé, 1975). Balascio et al. (2005a) also found a similar gradient in the Brooks Range, showing a clear rise in LGM ELAs from the west to the east. Studies from the Ahklun Mountains also reported a similar eastward rise in ELAs (Briner and Kaufman, 2000; Manley et al., 1997). The correlation between longitude and LIA ELA suggests that a similar gradient was present during both the LIA and LGM, with mountain ranges receiving less precipitation with increasing distance from the most probable moisture sources for our study areas in Alaska – the southern Bering Sea and northernmost Pacific Ocean. Precipitation from the Arctic Ocean was blocked by perennial sea ice during both the LGM and the LIA and moisture moving northward from the Gulf of Alaska was influenced by the rain shadow created by the Cordilleran Ice Sheet and/or the southern flanks of Alaska Range, effectively eliminating other potential sources of precipitation to our study sites (Briner and Kaufman, 2008; Balascio et al., 2005a; Péwé, 1975; Kienholz et al., 2015; Molnia, 2008). Interestingly, these gradients persisted during periods when the Bering Strait was both open and closed, suggesting that prevailing moisture sources did not differ greatly between the LGM and LIA. What remains unclear is if, and how, this LGM gradient would change with the inclusion of ELAs from southern southeastern Alaska. We might expect LGM ELAs to be lower here due to the proximity to the Pacific; however, the area was covered by the Cordilleran Ice Sheet until well after the LGM, and thus, we are unable to calculate ELAs here (Hamilton, 1994; Péwé, 1975; Walcott et al., 2022; Lesnek et al., 2020; Lesnek et al., 2018).

https://doi.org/10.5194/cp-2023-20
Preprint. Discussion started: 12 April 2023

5.3 Records of LGM paleoclimate

For nearly a century, researchers have attributed the relatively limited LGM glaciation in Alaska to increased aridity and relatively warm temperatures, noting that Alaska was dissimilar to areas farther south that were completely covered by the Cordilleran and Laurentide ice sheets (Capps, 1932; Flint, 1943). This aridity has since been confirmed by numerous studies. A pollen record synthesis indicates Alaska received up to 125 mm less precipitation per year than modern at 25 ka and continued to receive reduced precipitation until 20 ka (Viau et al., 2008). Bartlein et al. (2011) synthesized pollen data and suggested LGM annual precipitation was ~50 to 200 mm/yr lower than at present. More recent pollen studies (not included in these syntheses) confirm this, with records from lakes in the Brooks Range and the Yukon-Tanana Uplands both indicating increased aridity in Alaska during the LGM (Finkenbinder et al., 2014; Abbott et al., 2010). Additionally, geochemical analyses of sediment from Burial Lake near the Brooks Range show high magnetic concentrations and a dearth of organic matter during the LGM, suggesting a dry, windy environment with increased amounts of aeolian material deposited (Dorfman et al., 2015; Finkenbinder et al., 2015). Investigation of the $\delta^{18}O$ values from chironomids in the same sediments corroborate this, indicating a dry environment during the LGM (King et al., 2022) Finally, a lack of loess records across Alaska dating to the LGM is attributed to a dearth of vegetation to support loess deposition in turn caused by increased aridity statewide (Muhs et al., 2003).

A data assimilation product created with a collection of sea surface temperature data and an isotope-enabled climate model show annual precipitation differences of ca. -300 mm/yr during the LGM relative to the pre-industrial period, corroborating paleoclimate records of aridity (Tierney et al., 2020b; Tierney et al., 2020a). Climate model results corroborate this, showing a

https://doi.org/10.5194/cp-2023-20
Preprint. Discussion started: 12 April 2023

range of pre-industrial to LGM annual precipitation deficits between -150 and -600 mm/yr (Löfverström et al., 2014; Löfverström and Liakka, 2016). These proxy, data assimilation, and modeling studies justify our use of modern lapse rates and the dry adiabatic lapse rate to calculate maximum and minimum LGM summertime temperature depressions, respectively. Because Alaska was drier than today during the LGM, the LGM environmental lapse rate is unlikely to have been smaller than the modern lapse rates, nor would it be exceed the dry adiabatic lapse rate for any significant period of time (i.e., maximum of hours; Kaser and Osmaston, 2002).

Last Glacial Maximum summer temperature records are sparser, yet those created through paleoclimate proxies, data assimilation, and models all suggest that summertime temperatures in Alaska were just a few degrees colder during the LGM than the LIA or modern. Syntheses of pollen records shows mean summertime temperatures between -2 and -5 ºC colder than modern during the LGM. (Viau et al., 2008; Bartlein et al., 2011). Similarly, chironomid-inferred summer temperature records from lakes in western Alaska yield LGM temperature reconstructions ca. -3.5 ºC below modern (Kurek et al., 2009). This is substantiated further by a leaf wax hydrogen isotope temperature reconstruction from the central Brooks Range that indicates the LGM summers ca. -3 ºC cooler than the LIA (Daniels et al., 2021). Though these records represent small, isolated geographic areas, their agreement substantiates only modest summer LGM temperature depression across Alaska.

Our relatively low small summer temperature depressions are also corroborated by recent data assimilation studies. A data assimilation product of sea surface temperatures and isotope-enabled climate models shows summer temperature depressions across our study area of ca. -3.6 ºC during the LGM, relative to the pre-industrial period (Tierney et al., 2020a). This is slightly less

https://doi.org/10.5194/cp-2023-20
Preprint. Discussion started: 12 April 2023

Climate of the Past
Discussions

than our range of average maximum summer temperature depressions between -1.4 ± 0.8 ºC and -2.2 ± 1.1 ºC but agree well with our minimum summer temperature depressions of -3.4 ± 1.8 ºC.

Climate model results from a few studies vary, with some showing Alaska during the LGM a few degrees warmer than the pre-industrial (e.g., Otto-Bliesner et al., 2006), and others showing small LGM-LIA summer temperature depressions of -1 to -4 ºC (Löfverström et al., 2014; Löfverström and Liakka, 2016; Kageyama et al., 2021). These models indicate a clear pattern; Beringia was much warmer than other high latitude northern areas, such as the North Atlantic, though this magnitude of warming is not latitudinally congruent. Our data confirm this overall pattern of relatively warm summers in Beringia and highlight veracity of models that simulate mild temperature depressions across Alaska.

Our paleo-temperature data not only showcase the viability of calculating temperature depressions from ELAs reconstructions, but also provide further evidence of relatively mild LGM climate in Alaska. While proxy-derived average summer global temperature was -5 ± 2 ºC lower during the LGM, these were even lower in much of the high latitude areas of the Northern Hemisphere (outside of Alaska), with Arctic-average temperature depressions of -18 ± 7 ºC (Miller et al., 2010). Data assimilation results also indicate significant cooling in the much of the Arctic and a global mean temperature depression of ca. -5.7 to -6.5 ºC (Osman et al., 2021; Tierney et al., 2020a). Our range ΔELA-derived LGM maximum summer temperature depressions for Alaska of -1.4 ± 0.8 ºC and -2.2 ± 1.1 ºC are higher than reconstructed global temperature depressions. However, our minimum summer temperature depression estimate of -3.4 ± 1.8 ºC, is similar to the global average, but much greater than temperature depressions in the northern high latitudes suggesting that Arctic amplification was not zonally homogenous during the LGM.

5.4 Why was Alaska relatively dry and warm during the LGM?

Alaska was drier during the LGM than today, yet comparable LGM and LIA ELA gradients suggest similar moisture sources and suggest the importance of temperature as a control on glacier extent. The arid conditions in Alaska during the LGM have long been attributed to global eustatic sea level fall and the resultant emergence of the Bering Land Bridge, which has often been cited as a reason for relatively low ΔELAs in Alaska (Hopkins, 1982; Briner and Kaufman, 2008; Balascio et al., 2005a; Briner and Kaufman, 2000; Balascio et al., 2005b; Brigham-Grette, 2001; Elias et al., 1996). However, the similarity between LGM and LIA ELA gradients (i.e., with and without the presence of the Bering Land Bridge) suggests that the Bering Land Bridge did not play a major role in modulating precipitation during the LGM.

Syntheses of North Pacific sediment core records indicate lower sea surface temperatures during the end of the LGM (~20 – 19 ka), suggesting low moisture availability (Praetorius et al., 2018; Praetorius et al., 2020; Davis et al., 2020; Caissie et al., 2010). Much of the Bering Sea, North Pacific, and Arctic Ocean was covered by perennial sea ice during the LGM, further inhibiting moisture availability and precipitation in Alaska, and thus leading to lower ΔELAs there compared to the lower latitudes (Pelto et al., 2018; Sancetta et al., 1984; Polyak et al., 2010; Polyak et al., 2013; Caissie et al., 2010). However, while the southern Bering Sea and northernmost Pacific was largely free of sea ice during the LIA, the Arctic Ocean was still covered by perennial sea ice. This led to similar precipitation gradients as the LGM, with the southern Bering Sea and northernmost Pacific as the primary sources of moisture.

Relatively low summer temperature depressions in Alaska are also likely responsible for the limited ELA lowering in Alaska during the LGM. While a complete and satisfying mechanism for relatively warm summer temperatures in Alaska remains elusive, a growing number of

https://doi.org/10.5194/cp-2023-20
Preprint. Discussion started: 12 April 2023

Climate of the Past Discussions

modeling studies indicate the possibility that disruptions to global atmospheric circulation caused by large LGM ice sheets may help explain this phenomenon. In short, persistent anticyclonic circulation over the large North American ice sheets has two mechanistic impacts on atmospheric circulation and the regional radiation budget over Alaska in model simulations; (i) jet stream circulation becomes more meridional, and warm, southerly surface air is persistently advected into Alaska (e.g., Roe and Lindzen, 2001; Löfverström et al., 2014), and (ii) atmospheric subsidence driven by anticyclonic circulation inhibits local cloud formation increasing shortwave radiation in Alaska (e.g., Löfverström and Liakka, 2016; Löfverström et al., 2015). While model results are encouraging, the first mechanism is predominantly a wintertime phenomenon, and cloud dynamics are often sources of biases in models (e.g., Bony and Dufresne, 2005), so further analyses are likely required to test the hypothesis that large North American ice sheets modulated summer temperatures in Alaska during the LGM.

Because alpine glaciers are likely more sensitive to summer temperatures rather than annual temperatures, we suggest that the limited extents of alpine glaciers in Alaska and their correspondingly low ΔELAs were primarily due to relatively warm summers and also influenced by reduced annual precipitation (Rupper and Roe, 2008; Tulenko et al., 2020). We posit that the gradient of LGM ELAs seen across the state is largely controlled by precipitation. The lack of a western (Bering Land Bridge instead of the Bering Sea) or northern (sea ice cover over Chukchi Sea) moisture source, causes higher ELAs with increasing distance from the only available moisture source – the southern Bering Sea and northernmost Pacific. This gradient is especially pronounced in Alaska due LGM aridity; though temperature is the main driver of these LGM ELAs, any precipitation would have undoubtedly played a key role in the growth of any glaciers.

https://doi.org/10.5194/cp-2023-20
Preprint. Discussion started: 12 April 2023

6 Conclusions

- Maximum ΔELA-based summer temperature reconstructions of between ca. -1.4 ± 0.8 ºC and -2.2 ± 1.1 ºC, and minimum temperatures of -3.4 ± 1.8 ºC confirm recent marine proxy-based paleoclimate data assimilation studies that indicate Alaska experienced similar LGM temperature depressions to the global average. This contrasts with much of the high latitude areas of the Northern Hemisphere, where temperature depressions were much lower. These data agree with proxy and model studies that show slightly cooler LGM conditions in Alaska. They also highlight that Alaska experienced relatively small summer LGM temperature depressions to other northern high latitude areas, suggesting that Arctic amplification is not latitudinally congruent.
- LGM and LIA ELA reconstructions demonstrate similar gradients and statistically significant relationships between longitude and climate, indicating the influence of precipitation on glacier extent. The similarity of the gradient also suggests a similar moisture source during both the LGM and LIA and the lack of influence from the Bering Land Bridge.
- Future work should focus on modeling of LGM glaciers in Alaska to supplement ELA-based paleoclimate records, calculating hypothetical modern or LIA ELAs to calculate ΔELAs and temperature depressions statewide, and deriving ELAs and ΔELAs across the rest of Beringia (i.e., eastern Siberia) to assess paleoclimate conditions more broadly.

https://doi.org/10.5194/cp-2023-20
Preprint. Discussion started: 12 April 2023

Author Contributions

JPB, JPT, and CKW designed the study. JPB acquired funding. CKW conducted all GIS work and initial analysis. All coauthors contributed to discussion and further data analysis. CKW wrote the first draft of the manuscript; all coauthors provided edits and comments on subsequent drafts.

Competing Interests

The authors declare that they have no conflicts of interest.

Acknowledgements

We thank the National Science Foundation for funding this project under grant #1853705.

Data availability

ELA data and glacier extents generated in this study are included in the supplement.

https://doi.org/10.5194/cp-2023-20
Preprint. Discussion started: 12 April 2023

Climate of the Past Discussions

References

Abbott, M. B., Edwards, M. E., and Finney, B. P.: A 40,000-yr record of environmental change from Burial Lake in Northwest Alaska, Quaternary Research, 74, 156-165, doi:10.1016/j.yqres.2010.03.007, 2010.

Balascio, N. L., Kaufman, D. S., and Manley, W. F.: Equilibrium-line altitudes during the Last Glacial Maximum across the Brooks Range, Alaska, Journal of Quaternary Science: Published for the Quaternary Research Association, 20, 821-838, https://doi.org/10.1002/jqs.980, 2005a.

Balascio, N. L., Kaufman, D. S., Briner, J. P., and Manley, W. F.: Late Pleistocene glacial geology of the Okpilak-Kongakut rivers region, northeastern Brooks Range, Alaska, Arctic, Antarctic, and Alpine Research, 37, 416-424, 10.1657/1523-0430(2005)037[0416:LPGGOT]2.0.CO;2, 2005b.

Barclay, D. J., Wiles, G. C., and Calkin, P. E.: Holocene glacier fluctuations in Alaska, Quaternary Science Reviews, 28, 2034-2048, https://doi.org/10.1016/j.quascirev.2009.01.016, 2009.

Bartlein, P. J., Harrison, S. P., Brewer, S., Connor, S., Davis, B. A. S., Gajewski, K., Guiot, J., Harrison-Prentice, T. I., Henderson, A., and Peyron, O.: Pollen-based continental climate reconstructions at 6 and 21 ka: a global synthesis, Climate Dynamics, 37, 775-802, https://doi.org/10.1007/s00382-010-0904-1, 2011.

Benn, D. I. and Hulton, N. R. J.: An ExcelTM spreadsheet program for reconstructing the surface profile of former mountain glaciers and ice caps, Computers & Geosciences, 36, 605-610, https://doi.org/10.1016/j.cageo.2009.09.016, 2009.

Benn, D. I. and Lehmkuhl, F.: Mass balance and equilibrium-line altitudes of glaciers in high-mountain environments, Quaternary International, 65, 15-29, https://doi.org/10.1016/S1040-6182(99)00034-8, 2000.

Bony, S. and Dufresne, J.-L.: Marine boundary layer clouds at the heart of tropical cloud feedback uncertainties in climate models, Geophysical Research Letters, 32, https://doi.org/10.1029/2005GL023851, 2005.

Brigham-Grette, J.: New perspectives on Beringian Quaternary paleogeography, stratigraphy, and glacial history, Quaternary Science Reviews, 20, 15-24, https://doi.org/10.1016/S0277-3791(00)00134-7, 2001.

Briner, J. P. and Kaufman, D. S.: Late Pleistocene glaciation of the southwestern Ahklun mountains, Alaska, Quaternary Research, 53, 13-22, doi:10.1006/qres.1999.2088, 2000.

Briner, J. P. and Kaufman, D. S.: Late Pleistocene mountain glaciation in Alaska: key chronologies, Journal of Quaternary Science: Published for the Quaternary Research Association, 23, 659-670, https://doi.org/10.1002/jqs.1196, 2008.

Broecker, W. S. and Denton, G. H.: The role of ocean-atmosphere reorganizations in glacial cycles, Quaternary Science Reviews, 9, 305-341, https://doi.org/10.1016/0277-3791(90)90026-7, 1990.

Brooks, J. P., Larocca, L. J., and Axford, Y. L.: Little Ice Age climate in southernmost Greenland inferred from quantitative geospatial analyses of alpine glacier reconstructions, Quaternary Science Reviews, 293, 107701, https://doi.org/10.1016/j.quascirev.2022.107701, 2022.

Caissie, B. E., Brigham-Grette, J., Lawrence, K. T., Herbert, T. D., and Cook, M. S.: Last Glacial

Maximum to Holocene sea surface conditions at Umnak Plateau, Bering Sea, as inferred from diatom, alkenone, and stable isotope records, Paleoceanography, 25, https://doi.org/10.1029/2008PA001671, 2010.

Capps, S. R.: Glaciation in Alaska, 2330-7102, https://doi.org/10.3133/pp170A, 1932.

Coulter, H. W., Hopkins, D. M., Karlstrom, T. N. V., Pewe, T. L., Wahrhaftig, C., and Williams, J. R.: Map showing extent of glaciations in Alaska, Report 415, https://doi.org/10.3133/i415, 1965.

Daigle, T. A. and Kaufman, D. S.: Holocene climate inferred from glacier extent, lake sediment and tree rings at Goat Lake, Kenai Mountains, Alaska, USA, Journal of Quaternary Science: Published for the Quaternary Research Association, 24, 33-45, https://doi.org/10.1002/jqs.1166, 2009.

Daniels, W. C., Russell, J. M., Morrill, C., Longo, W. M., Giblin, A. E., Holland-Stergar, P., Welker, J. M., Wen, X., Hu, A., and Huang, Y.: Lacustrine leaf wax hydrogen isotopes indicate strong regional climate feedbacks in Beringia since the last ice age, Quaternary Science Reviews, 269, 107130, 2021.

Davis, C. V., Myhre, S. E., Deutsch, C., Caissie, B., Praetorius, S., Borreggine, M., and Thunell, R.: Sea surface temperature across the Subarctic North Pacific and marginal seas through the past 20,000 years: A paleoceanographic synthesis, Quaternary Science Reviews, 246, 106519, https://doi.org/10.1016/j.quascirev.2020.106519, 2020.

Dorfman, J. M., Stoner, J. S., Finkenbinder, M. S., Abbott, M. B., Xuan, C., and St-Onge, G.: A 37,000-year environmental magnetic record of aeolian dust deposition from Burial Lake, Arctic Alaska, Quaternary Science Reviews, 128, 81-97, https://doi.org/10.1016/j.quascirev.2015.08.018, 2015.

Dortch, J. M., Owen, L. A., Caffee, M. W., and Brease, P.: Late Quaternary glaciation and equilibrium line altitude variations of the McKinley River region, central Alaska Range, Boreas, 39, 233-246, https://doi.org/10.1111/j.1502-3885.2009.00121.x, 2010.

Elias, S. A., Short, S. K., Nelson, C. H., and Birks, H. H.: Life and times of the Bering land bridge, Nature, 382, 60-63, https://doi.org/10.1038/382060a0 1996.

Federici, P. R., Granger, D. E., Pappalardo, M., Ribolini, A., Spagnolo, M., and Cyr, A. J.: Exposure age dating and Equilibrium Line Altitude reconstruction of an Egesen moraine in the Maritime Alps, Italy, Boreas, 37, 245-253, https://doi.org/10.1111/j.1502-3885.2007.00018.x, 2008.

Finkenbinder, M. S., Abbott, M. B., Finney, B. P., Stoner, J. S., and Dorfman, J. M.: A multi-proxy reconstruction of environmental change spanning the last 37,000 years from Burial Lake, Arctic Alaska, Quaternary Science Reviews, 126, 227-241, https://doi.org/10.1016/j.quascirev.2015.08.031, 2015.

Finkenbinder, M. S., Abbott, M. B., Edwards, M. E., Langdon, C. T., Steinman, B. A., and Finney, B. P.: A 31,000 year record of paleoenvironmental and lake-level change from Harding Lake, Alaska, USA, Quaternary Science Reviews, 87, 98-113, https://doi.org/10.1016/j.quascirev.2014.01.005, 2014.

Flint, R. F.: Growth of North American Ice Sheet During the Wisconsin Age, GSA Bulletin, 54, 325-362, 10.1130/GSAB-54-325, 1943.

Hamilton, T. D.: Late Cenozoic glaciation of Alaska, 10.1130/DNAG-GNA-G1.813, 1994.

Hamilton, T. D. and Porter, S. C.: Itkillik Glaciation in the Brooks Range, Northern Alaska, Quaternary Research, 5, 471-497, 10.1016/0033-5894(75)90012-5, 1975.

Haugen, R. K., Lynch, M. J., and Roberts, T. C.: Summer Temperatures in Interior Alaska,

Research report (Cold Regions Research and Engineering Laboratory (U.S.))), Corps of Engineers, U.S. Army Cold Regions Research and Engineering Laboratory, 1971.
Hopkins, D. M.: Aspects of the paleogeography of Beringia during the late Pleistocene, Paleoecology of Beringia, 3-28, https://doi.org/10.1016/B978-0-12-355860-2.50008-9, 1982.
Kageyama, M., Harrison, S. P., Kapsch, M. L., Lofverstrom, M., Lora, J. M., Mikolajewicz, U., Sherriff-Tadano, S., Vadsaria, T., Abe-Ouchi, A., Bouttes, N., Chandan, D., Gregoire, L. J., Ivanovic, R. F., Izumi, K., LeGrande, A. N., Lhardy, F., Lohmann, G., Morozova, P. A., Ohgaito, R., Paul, A., Peltier, W. R., Poulsen, C. J., Quiquet, A., Roche, D. M., Shi, X., Tierney, J. E., Valdes, P. J., Volodin, E., and Zhu, J.: The PMIP4 Last Glacial Maximum experiments: preliminary results and comparison with the PMIP3 simulations, Clim. Past, 17, 1065-1089, 10.5194/cp-17-1065-2021, 2021.
Kaser, G. and Osmaston, H.: Tropical glaciers, Cambridge University Press, 2002.
Kaufman, D. S. and Hopkins, D. M.: Glacial history of the Seward Peninsula, 1986.
Kaufman, D. S., Young, N. E., Briner, J. P., and Manley, W. F.: Alaska palaeo-glacier atlas (version 2), in: Developments in Quaternary Sciences, Elsevier, 427-445, https://doi.org/10.1016/B978-0-444-53447-7.00033-7, 2011.
Kienholz, C., Herreid, S., Rich, J. L., Arendt, A. A., Hock, R., and Burgess, E. W.: Derivation and analysis of a complete modern-date glacier inventory for Alaska and northwest Canada, Journal of Glaciology, 61, 403-420, 10.3189/2015JoG14J230, 2015.
King, A. L., Anderson, L., Abbott, M., Edwards, M., Finkenbinder, M. S., Finney, B., and Wooller, M. J.: A stable isotope record of late Quaternary hydrologic change in the northwestern Brooks Range, Alaska (eastern Beringia), Journal of Quaternary Science, 37, 928-943, https://doi.org/10.1002/jqs.3368, 2022.
Kłapyta, P., Mîndrescu, M., and Zasadni, J.: Geomorphological record and equilibrium line altitude of glaciers during the last glacial maximum in the Rodna Mountains (eastern Carpathians), Quaternary Research, 100, 1-20, 10.1017/qua.2020.90, 2021.
Kurek, J., Cwynar, L. C., Ager, T. A., Abbott, M. B., and Edwards, M. E.: Late Quaternary paleoclimate of western Alaska inferred from fossil chironomids and its relation to vegetation histories, Quaternary Science Reviews, 28, 799-811, https://doi.org/10.1016/j.quascirev.2008.12.001, 2009.
Kurowski, L.: Die Höhe der Schneegrenze mit Besonderer Berücksichtigung der Finsteraarhorn-Gruppe, Pencks Geographische Abhandlungen 5, 1891.
Leonard, E. M., Laabs, B. J. C., Plummer, M. A., Kroner, R. K., Brugger, K. A., Spiess, V. M., Refsnider, K. A., Xia, Y., and Caffee, M. W.: Late Pleistocene glaciation and deglaciation in the Crestone Peaks area, Colorado Sangre de Cristo Mountains, USA – chronology and paleoclimate, Quaternary Science Reviews, 158, 127-144, https://doi.org/10.1016/j.quascirev.2016.11.024, 2017.
Lesnek, A. J., Briner, J. P., Baichtal, J. F., and Lyles, A. S.: New constraints on the last deglaciation of the Cordilleran Ice Sheet in coastal Southeast Alaska, Quaternary Research, 96, 140-160, doi:10.1017/qua.2020.32, 2020.
Lesnek, A. J., Briner, J. P., Lindqvist, C., Baichtal, J. F., and Heaton, T. H.: Deglaciation of the Pacific coastal corridor directly preceded the human colonization of the Americas, Science Advances, 4, eaar5040, 10.1126/sciadv.aar5040 %J Science Advances, 2018.
Levy, L. B., Kaufman, D. S., and Werner, A.: Holocene glacier fluctuations, Waskey Lake,

northeastern Ahklun mountains, southwestern Alaska, The Holocene, 14, 185-193, https://doi.org/10.1191/0959683604hl675rp, 2004.
Löfverström, M. and Liakka, J.: On the limited ice intrusion in Alaska at the LGM, Geophysical Research Letters, 43, 11-030, https://doi.org/10.1002/2016GL071012, 2016.
Löfverström, M., Liakka, J., and Kleman, J.: The North American Cordillera—An Impediment to Growing the Continent-Wide Laurentide Ice Sheet, Journal of Climate, 28, 9433-9450, https://doi.org/10.1175/JCLI-D-15-0044.1, 2015.

Löfverström, M., Caballero, R., Nilsson, J., and Kleman, J.: Evolution of the large-scale atmospheric circulation in response to changing ice sheets over the last glacial cycle, Climate of the Past, 10, 1453-1471, https://doi.org/10.5194/cp-10-1453-2014, 2014.
Manley, W., Kaufman, D., and Briner, J.: GIS determination of late Wisconsin equilibrium line altitudes in the Ahklun Mountains of southwestern Alaska, Geological Society of America Abstracts with Programs, A33, 1997.
Mann, D. H. and Peteet, D. M.: Extent and Timing of the Last Glacial Maximum in Southwestern Alaska, Quaternary Research, 42, 136-148, https://doi.org/10.1006/qres.1994.1063, 1994.
McKay, N. P. and Kaufman, D. S.: Holocene climate and glacier variability at Hallet and Greyling Lakes, Chugach Mountains, south-central Alaska, Journal of Paleolimnology, 41, 143-159, https://doi.org/10.1007/s10933-008-9260-0, 2009.
Millan, R., Mouginot, J., Rabatel, A., and Morlighem, M.: Ice velocity and thickness of the world's glaciers, Nature Geoscience, 15, 124-129, https://doi.org/10.1038/s41561-021-00885-z, 2022.
Miller, G. H., Alley, R. B., Brigham-Grette, J., Fitzpatrick, J. J., Polyak, L., Serreze, M. C., and White, J. W. C.: Arctic amplification: can the past constrain the future?, Quaternary Science Reviews, 29, 1779-1790, https://doi.org/10.1016/j.quascirev.2010.02.008, 2010.
Mitchell, S. G. and Humphries, E. E.: Glacial cirques and the relationship between equilibrium line altitudes and mountain range height, Geology, 43, 35-38, 10.1130/G36180.1, 2015.
Molnia, B. F.: Glaciers of North America - Glaciers of Alaska, Report 1386K, 10.3133/pp1386K, 2008.
Muhs, D. R., Ager, T. A., Arthur Bettis, E., McGeehin, J., Been, J. M., Begét, J. E., Pavich, M. J., Stafford, T. W., and Stevens, D. A. S. P.: Stratigraphy and palaeoclimatic significance of Late Quaternary loess–palaeosol sequences of the Last Interglacial–Glacial cycle in central Alaska, Quaternary Science Reviews, 22, 1947-1986, https://doi.org/10.1016/S0277-3791(03)00167-7, 2003.
Nesje, A.: Reconstructing Paleo ELAs on Glaciated Landscapes, in: Reference Module in Earth Systems and Environmental Sciences, Elsevier, https://doi.org/10.1016/B978-0-12-409548-9.09425-2, 2014.
Ohmura, A. and Boettcher, M.: Climate on the equilibrium line altitudes of glaciers: theoretical background behind Ahlmann's P/T diagram, Journal of Glaciology, 64, 489-505, https://doi.org/10.1017/jog.2018.41, 2018.
Ohmura, A., Kasser, P., and Funk, M.: Climate at the equilibrium line of glaciers, Journal of Glaciology, 38, 397-411, doi:10.3189/S0022143000002276, 1992.
Oien, R. P., Rea, B. R., Spagnolo, M., Barr, I. D., and Bingham, R. G.: Testing the area–altitude balance ratio (AABR) and accumulation–area ratio (AAR) methods of calculating glacier equilibrium-line altitudes, Journal of Glaciology, 1-12, doi:10.1017/jog.2021.100, 2021.

https://doi.org/10.5194/cp-2023-20
Preprint. Discussion started: 12 April 2023

Climate of the Past Discussions

Ono, Y., Aoki, T., Hasegawa, H., and Dali, L.: Mountain glaciation in Japan and Taiwan at the global Last Glacial Maximum, Quaternary international, 138, 79-92, https://doi.org/10.1016/j.quaint.2005.02.007, 2005.
Osman, M. B., Tierney, J. E., Zhu, J., Tardif, R., Hakim, G. J., King, J., and Poulsen, C. J.: Globally resolved surface temperatures since the Last Glacial Maximum, Nature, 599, 239-244, 10.1038/s41586-021-03984-4, 2021.
Otto-Bliesner, B. L., Brady, E. C., Clauzet, G., Tomas, R., Levis, S., and Kothavala, Z.: Last glacial maximum and Holocene climate in CCSM3, Journal of Climate, 19, 2526-2544, https://doi.org/10.1175/JCLI3748.1 2006.
Pellitero, R., Rea, B. R., Spagnolo, M., Bakke, J., Hughes, P., Ivy-Ochs, S., Lukas, S., and Ribolini, A.: A GIS tool for automatic calculation of glacier equilibrium-line altitudes, Computers & Geosciences, 82, 55-62, https://doi.org/10.1016/j.cageo.2015.05.005, 2015.
Pellitero, R., Rea, B. R., Spagnolo, M., Bakke, J., Ivy-Ochs, S., Frew, C. R., Hughes, P., Ribolini, A., Lukas, S., and Renssen, H.: GlaRe, a GIS tool to reconstruct the 3D surface of palaeoglaciers, Computers & Geosciences, 94, 77-85, https://doi.org/10.1016/j.cageo.2016.06.008, 2016.
Pelto, B. M., Caissie, B. E., Petsch, S. T., and Brigham-Grette, J.: Oceanographic and Climatic Change in the Bering Sea, Last Glacial Maximum to Holocene, Paleoceanography and Paleoclimatology, 33, 93-111, https://doi.org/10.1002/2017PA003265, 2018.
Péwé, T. L.: Multiple glaciation in Alaska: a progress report, US Department of the Interior, Geological Survey, 1953.
Péwé, T. L.: Quaternary geology of Alaska, Report 835, 10.3133/pp835, 1975.
Plummer, M. A. and Phillips, F. M.: A 2-D numerical model of snow/ice energy balance and ice flow for paleoclimatic interpretation of glacial geomorphic features, Quaternary Science Reviews, 22, 1389-1406, https://doi.org/10.1016/S0277-3791(03)00081-7, 2003.
Polyak, L., Best, K. M., Crawford, K. A., Council, E. A., and St-Onge, G.: Quaternary history of sea ice in the western Arctic Ocean based on foraminifera, Quaternary Science Reviews, 79, 145-156, https://doi.org/10.1016/j.quascirev.2012.12.018, 2013.
Polyak, L., Alley, R. B., Andrews, J. T., Brigham-Grette, J., Cronin, T. M., Darby, D. A., Dyke, A. S., Fitzpatrick, J. J., Funder, S., Holland, M., Jennings, A. E., Miller, G. H., O'Regan, M., Savelle, J., Serreze, M., St. John, K., White, J. W. C., and Wolff, E.: History of sea ice in the Arctic, Quaternary Science Reviews, 29, 1757-1778, https://doi.org/10.1016/j.quascirev.2010.02.010, 2010.
Porter, S. C.: Some Geological Implications of Average Quaternary Glacial Conditions, Quaternary Research, 32, 245-261, 10.1016/0033-5894(89)90092-6, 1989.
Praetorius, S., Rugenstein, M., Persad, G., and Caldeira, K.: Global and Arctic climate sensitivity enhanced by changes in North Pacific heat flux, Nature Communications, 9, 3124, 10.1038/s41467-018-05337-8, 2018.
Praetorius, S. K., Condron, A., Mix, A. C., Walczak, M. H., McKay, J. L., and Du, J.: The role of Northeast Pacific meltwater events in deglacial climate change, Science Advances, 6, eaay2915, 10.1126/sciadv.aay2915, 2020.
Rea, B. R., Pellitero, R., Spagnolo, M., Hughes, P., Ivy-Ochs, S., Renssen, H., Ribolini, A., Bakke, J., Lukas, S., and Braithwaite, R. J.: Atmospheric circulation over Europe during the Younger Dryas, Science Advances, 6, eaba4844, doi:10.1126/sciadv.aba4844, 2020.
Rodbell, D. T.: Late Pleistocene equilibrium-line reconstructions in the northern Peruvian Andes, Boreas, 21, 43-52, https://doi.org/10.1111/j.1502-3885.1992.tb00012.x, 1992.

https://doi.org/10.5194/cp-2023-20
Preprint. Discussion started: 12 April 2023

Climate of the Past
Open Access
Discussions

Roe, Gerard H., Baker, Marcia B., and Herla, F.: Centennial glacier retreat as categorical evidence of regional climate change, Nature Geoscience, 10, 95-99, 10.1038/ngeo2863, 2017.

Roe, G. H. and Lindzen, R. S.: The Mutual Interaction between Continental-Scale Ice Sheets and Atmospheric Stationary Waves, Journal of Climate, 14, 1450-1465, https://doi.org/10.1175/1520-0442(2001)014<1450:TMIBCS>2.0.CO;2, 2001.

Rupper, S. and Roe, G.: Glacier changes and regional climate: A mass and energy balance approach, Journal of Climate, 21, 5384-5401, https://doi.org/10.1175/2008JCLI2219.1, 2008.

Sancetta, C., Heusser, L., Labeyrie, L., Naidu, A. S., and Robinson, S. W.: Wisconsin—Holocene paleoenvironment of the Bering Sea: Evidence from diatoms, pollen, oxygen isotopes and clay minerals, Marine Geology, 62, 55-68, https://doi.org/10.1016/0025-3227(84)90054-9 1984.

Sikorski, J. J., Kaufman, D. S., Manley, W. F., and Nolan, M.: Glacial-geologic evidence for decreased precipitation during the Little Ice Age in the Brooks Range, Alaska, Arctic, Antarctic, and Alpine Research, 41, 138-150, https://doi.org/10.1657/1523-0430-41.1.138, 2009.

Solomina, O. N., Bradley, R. S., Hodgson, D. A., Ivy-Ochs, S., Jomelli, V., Mackintosh, A. N., Nesje, A., Owen, L. A., Wanner, H., Wiles, G. C., and Young, N. E.: Holocene glacier fluctuations, Quaternary Science Reviews, 111, 9-34, https://doi.org/10.1016/j.quascirev.2014.11.018, 2015.

Stansell, N. D., Polissar, P. J., and Abbott, M. B.: Last glacial maximum equilibrium-line altitude and paleo-temperature reconstructions for the Cordillera de Mérida, Venezuelan Andes, Quaternary Research, 67, 115-127, doi:10.1016/j.yqres.2006.07.005, 2007.

Sutherland, D. G.: Modern glacier characteristics as a basis for inferring former climates with particular reference to the Loch Lomond Stadial, Quaternary Science Reviews, 3, 291-309, https://doi.org/10.1016/0277-3791(84)90010-6, 1984.

Tierney, J. E., Zhu, J., King, J., Malevich, S. B., Hakim, G. J., and Poulsen, C. J.: Glacial cooling and climate sensitivity revisited, Nature, 584, 569-573, 10.1038/s41586-020-2617-x, 2020a.

Tierney, J. E., Poulsen, C. J., Montañez, I. P., Bhattacharya, T., Feng, R., Ford, H. L., Hönisch, B., Inglis, G. N., Petersen, S. V., and Sagoo, N.: Past climates inform our future, Science, 370, 10.1126/science.aay3701, 2020b.

Tulenko, J. P., Lofverstrom, M., and Briner, J. P.: Ice sheet influence on atmospheric circulation explains the patterns of Pleistocene alpine glacier records in North America, Earth and Planetary Science Letters, 534, 116115, https://doi.org/10.1016/j.epsl.2020.116115, 2020.

Tulenko, J. P., Briner, J. P., Young, N. E., and Schaefer, J. M.: Beryllium-10 chronology of early and late Wisconsinan moraines in the Revelation Mountains, Alaska: Insights into the forcing of Wisconsinan glaciation in Beringia, Quaternary Science Reviews, 197, 129-141, https://doi.org/10.1016/j.quascirev.2018.08.009, 2018.

Verbyla, D. and Kurkowski, T. A.: NDVI–Climate relationships in high-latitude mountains of Alaska and Yukon Territory, Arctic, Antarctic, and Alpine Research, 51, 397-411, 10.1080/15230430.2019.1650542, 2019.

Viau, A. E., Gajewski, K., Sawada, M. C., and Bunbury, J.: Low-and high-frequency climate variability in eastern Beringia during the past 25 000 years, Canadian Journal of Earth Sciences, 45, 1435-1453, https://doi.org/10.1139/E08-036, 2008.

https://doi.org/10.5194/cp-2023-20
Preprint. Discussion started: 12 April 2023

Climate of the Past
Discussions

Walcott, C. K.: GIS reconstructions of former glaciers shed light on past climate, Nature Reviews Earth & Environment, 3, 292-292, https://doi.org/10.1038/s43017-022-00293-w, 2022.

Walcott, C. K., Briner, J. P., Baichtal, J. F., Lesnek, A. J., and Licciardi, J. M.: Cosmogenic ages indicate no MIS 2 refugia in the Alexander Archipelago, Alaska, Geochronology, 4, 191-211, 10.5194/gchron-4-191-2022, 2022.

Zemp, M., Huss, M., Thibert, E., Eckert, N., McNabb, R., Huber, J., Barandun, M., Machguth, H., Nussbaumer, S. U., Gärtner-Roer, I., Thomson, L., Paul, F., Maussion, F., Kutuzov, S., and Cogley, J. G.: Global glacier mass changes and their contributions to sea-level rise from 1961 to 2016, Nature, 568, 382-386, 10.1038/s41586-019-1071-0, 2019.

https://doi.org/10.5194/cp-2023-20
Preprint. Discussion started: 12 April 2023

Climate of the Past
Discussions
Open Access
EGU

Figures

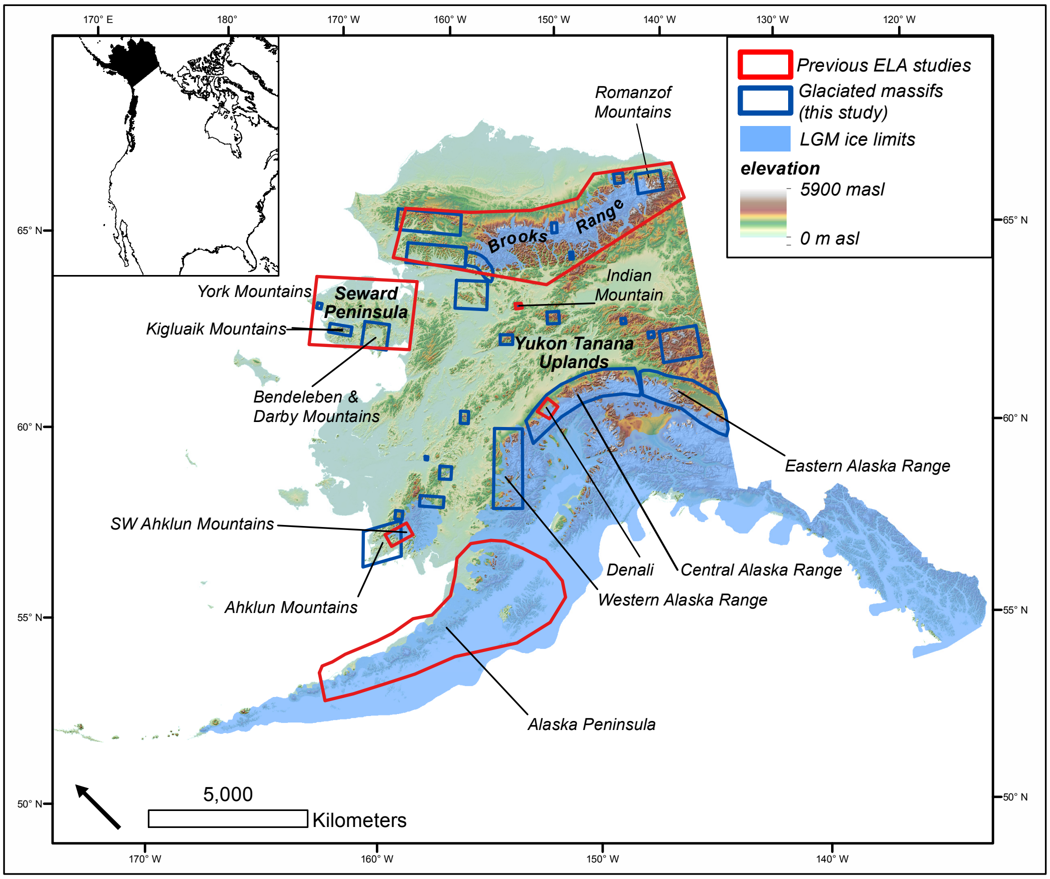

Figure 1. Map of Alaska with LGM ice limits (light blue; http://akatlas.geology.buffalo.edu/; date of last access: 1/4/23; Kaufman et al., 2011). Glaciated massifs used in this study outlined in dark blue boxes. Previous studies highlighted with reported ΔELAs in red: Brooks Range (Hamilton and Porter, 1975; Balascio et al., 2005), Seward Peninsula (Kaufman and Hopkins, 1986), Indian Mountain (Péwé, 1975), Denali (Dortch et al., 2010), SW Ahklun Mountains (Briner and Kaufman 2000), Alaska Peninsula (Mann and Peteet, 1994).

https://doi.org/10.5194/cp-2023-20
Preprint. Discussion started: 12 April 2023

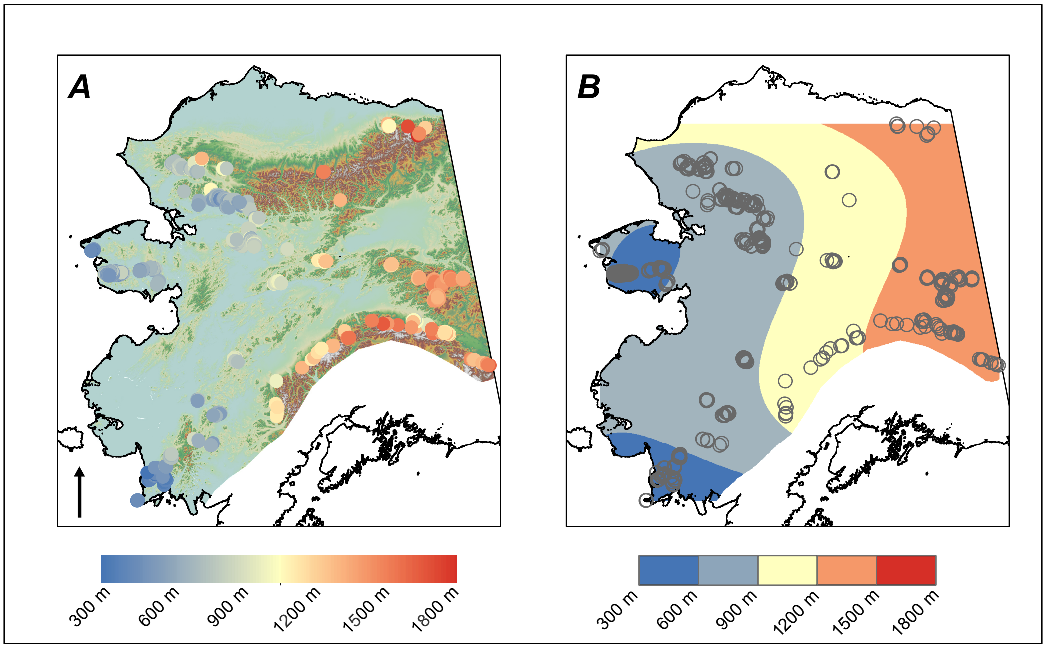

Figure 2. A) AAR LGM ELAs for all 480 reconstructed LGM glaciers plotted on a color gradient. Blue are glaciers with lower ELAs; red, higher ELAs. Areas of Cordilleran Ice Sheet influence are excluded from the map. **B)** Polynomial trend surface (3rd order) of LGM ELAs. Again, blue and red are low and high LGM ELAs, respectively.

https://doi.org/10.5194/cp-2023-20
Preprint. Discussion started: 12 April 2023

Climate of the Past
Discussions
Open Access
EGU

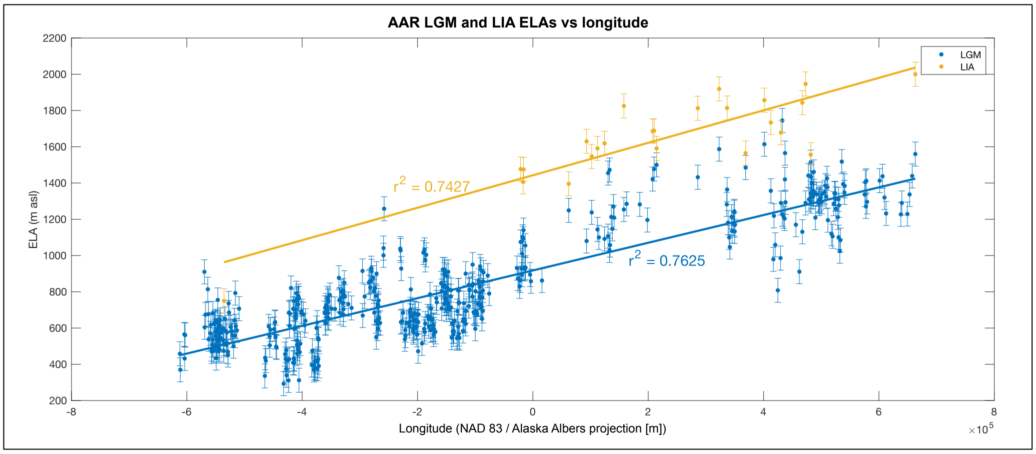

Figure 3. AAR LGM (blue) and LIA (yellow) ELAs plotted against longitude with lines of best fit.

https://doi.org/10.5194/cp-2023-20
Preprint. Discussion started: 12 April 2023

Climate of the Past
Discussions
Open Access

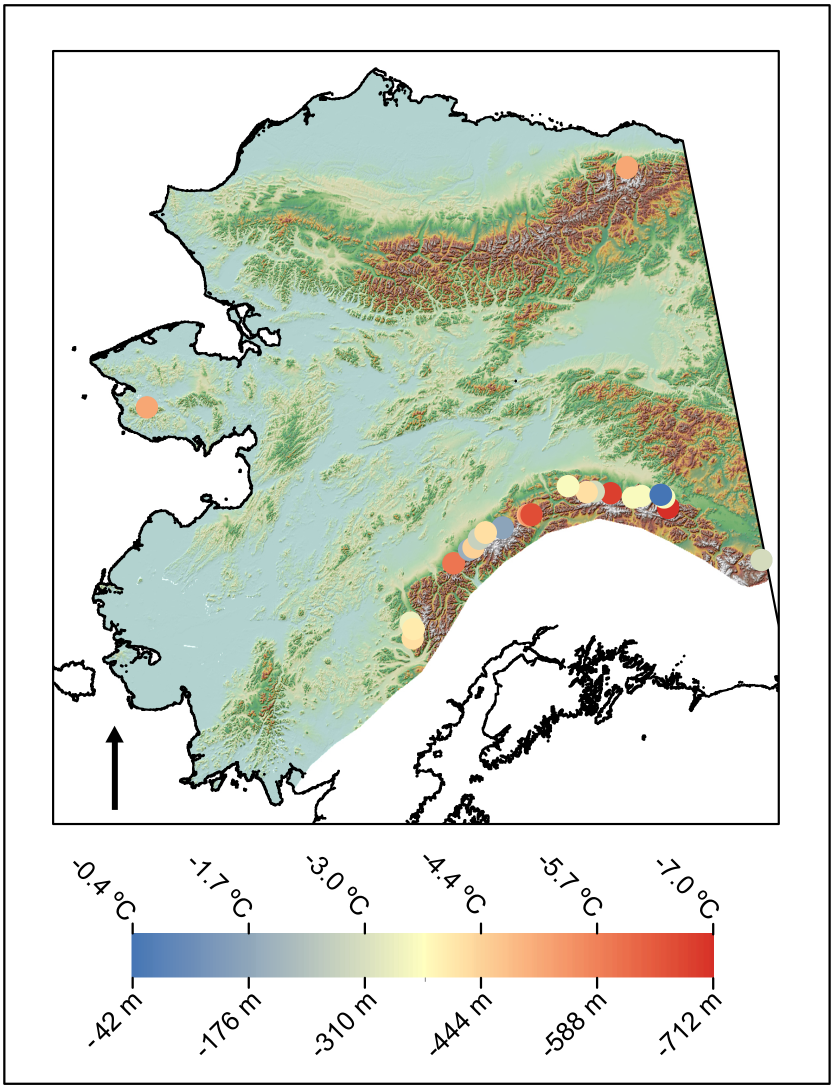

Figure 4: LGM - LIA ΔELAs and ΔELA-derived minimum summer temperature depressions calculated with the dry adiabatic lapse rate. Blue dots show little LGM ELA lowering (higher temperature depressions), while red dots show large amounts of ELA lowering (lower temperature depressions). Areas of Cordilleran Ice Sheet influence are excluded from the map. Note that the greatest ΔELA is < -750 m.